A 40-year retrospective European radon flux inventory including climatological variability

I. López-Coto [a,*], J.L. Mas [b], J.P. Bolivar [a]

[a] Dept. of Applied Physics, University of Huelva, 21071 Huelva, Spain
[b] Dept. of Applied Physics I, University of Seville, 41012 Seville, Spain

HIGHLIGHTS

- 40-year retrospective high-resolution European Rn flux inventory has been calculated.
- A model of radon transport in the earth crust allow us to calculate the soil fluxes.
- Mean values, probability distributions and seasonal fluctuations have been obtained.
- The results show wide variations depending on location and season of the year.
- The inventory can be easily integrated into atmospheric transport models.

ARTICLE INFO

Article history:
Received 2 February 2012
Received in revised form
19 February 2013
Accepted 22 February 2013

Keywords:
Radon flux
Exhalation
European radon inventory
Climatological variability
Numerical simulations

ABSTRACT

In this work, a 40-year retrospective European radon flux inventory has been calculated. Average values of the radon exhalation rate, probability distributions and seasonal fluctuations have been obtained. To achieve this, a numerical model of radon transport through finite, heterogeneous and porous media has been implemented, enabling us to calculate the radon exhalation rate of European soils with a horizontal resolution of 0.5′ (~1 km). Geological, geochemical and climatological parameters derived from European and international databases (FOREGS, HWSD, ERA-40) have been coupled to the model.

The theoretical model is based on the fundamental equation of radon transport in porous media, taking into account the dependency of the transport coefficient on temperature and humidity. It also includes a simple model that evaluates the effect of snow cover. In general, the results show wide variations depending on location and season of the year, with a spatial standard deviation close to the annual average value (30 Bq m^{-2} h^{-1}) In turn, the seasonal deviation is about 25% of the annual average value.

The inventory can be easily integrated into atmospheric transport models acting as baseline that could be used for policy decisions regarding the identification of areas with a high risk of exposure to radon. The gridded data are available for the scientific community upon request. The limitations and sources of errors and uncertainties of the model are also discussed in detail.

1. Introduction

The natural radioactive noble gas radon, ^{222}Rn, is mainly terrestrial in origin and is dispersed in the air by atmospheric transport and mixing. Radon is a noble gas suffering no deposition, washout nor chemical reactions. The only loss mechanism is radioactive decay, so the residence time of radon in the atmosphere is well-known. Hence, the radioactive gas ^{222}Rn has been widely used to evaluate atmospheric transport models (Jacob et al., 1997; Dentener et al., 1999), and by inverting these models, the location, extent and magnitude of sources and sinks of greenhouse gases can be determined (Gurney et al., 2002; Bousquet et al., 2006).

Currently, the effective use of ^{222}Rn in this context is limited by the accuracy of inventories of emissions into the atmosphere, which are scarce and based on simple assumptions and low spatial resolution. Furthermore, they do not account for the effects associated to weather conditions, which play an important role due to the fact that the radon transport coefficient depends heavily on the content of soil humidity (Rasch et al., 2000; Conen and Robertson, 2002).

A more accurate inventory at European level has been described in Szegvary et al. (2009), based on experimental correlations

* Corresponding author.
E-mail address: israel.lopez@dfa.uhu.es (I. López-Coto).

1352-2310/$ – see front matter http://dx.doi.org/10.1016/j.atmosenv.2013.02.043

between the radon exhalation rate and the external gamma radiation exposure.

A different approach was adopted by Schery and Wasiolek (1998), who propose combining the calculation of radon exhalation rate from a transport model in porous media and its calibration through experimental measurements in order to obtain the parameters that govern the flow in the subsurface. The limitation of this methodology lies in the applicability associated with the local calibration of the model, which cannot be extrapolated to other geographic areas.

A new inventory based on this idea has recently been published by Griffiths et al. (2010), who present an exhalation map for Australia with a spatial resolution of 0.05° (~5.5 km) and temporal resolution of one month based on the inclusion of geophysical and geochemical parameters of soil and weather conditions in a transport model. However, the authors have based their solution on an analytical approach to the general transport equation, which incorporates a linear combination of solutions for different layers. This implies that the numerical solution is not complete due to the mathematical expansion of the diffusive term when the diffusion coefficient is not uniform throughout the soil profile. In this way, the exhalation rate predicted by the model could be underestimated.

With these considerations in mind, the aim of this work was to implement a transport model of radon in porous, heterogeneous media based on the underlying transport equation. The model is solved by using numerical techniques in order to obtain an inventory of radon emissions into the atmosphere in Europe, with high spatial resolution and dependent on weather variables, which can be easily integrated into atmospheric transport models.

2. Theoretical framework review

Atoms of radon emanated from the material grains are distributed between the different phases in the media: air, water and solid. In each of these, mass transport is driven by advective and diffusive fluxes, biased by terms of generation (source) and annihilation (sink). Therefore, modelling of radon transport in porous materials requires the consideration of the continuity equations of the radon concentration for each phase, taking into account the exchange terms between them (Nazaroff and Nero, 1988; Porstendöfer, 1994).

The complexity of the problem can be reduced by transforming the transport equations for each phase into an equivalent equation for a single phase, air from the interstitial volume, using expanded definitions of the diffusion coefficient, permeability and porosity (Rogers and Nielson, 1991). These expanded magnitudes are identified by the term "effective", performing the coupling between phases.

$$\beta\frac{\partial C_{\mathrm{Rn}}}{\partial t} = \nabla\cdot\left(D_b\nabla C_{\mathrm{Rn}} + \frac{K}{\mu}\nabla P C_{\mathrm{Rn}}\right) - \beta\lambda_{\mathrm{Rn}}C_{\mathrm{Rn}} + \rho_b\varepsilon\lambda_{\mathrm{Rn}}C_{\mathrm{Ra}} \quad (1)$$

$$D_b = \beta D_e \quad (2)$$

$$\begin{aligned} L &= C_w/C_{\mathrm{Rn}} \\ k_a &= C_s/C_{\mathrm{Rn}} \\ \beta &= (1-s+sL)p + \rho_b k_a \\ s &= p_w/p \end{aligned} \quad (3)$$

where the subscript w is associated with the water phase, the subscript s refers to solid phase and the subscript Rn corresponds to the air phase.

β effective porosity
p Porosity
s humidity saturation
L Ostwald coefficient ($L = 0.2593$ at $T = 20$ °C)
k_a solid phase adsorption coefficient
ρ_b bulk density
D_b bulk diffusion coefficient
D_e effective diffusion coefficient
K permeability
μ air dynamic viscosity
P pressure field
λ_{Rn} ^{222}Rn decay constant ($2.098\cdot10^{-6}$ s^{-1})
C_{Rn} air ^{222}Rn concentration
ε emanation factor

The radon diffusion coefficient varies considerably depending on the moisture present in the soil and porosity. That dependence can be explicitly established according to empirical expressions (Rogers and Nielson, 1991):

$$D_e = D_0 p\exp\left(-6sp - 6s^{14p}\right) \quad (4)$$

D_0 being the radon diffusion coefficient in air, $1.1\cdot10^{-5}$ m^2 s^{-1}.

It is possible to estimate the value of the permeability by the following empirical equation (Rogers and Nielson, 1991).

$$K = \left(\frac{p}{110}\right)^2 d^{4/3}\exp\left(-12s^4\right) \quad (5)$$

where d is the mean grain diameter of the material.

In general, the advective flow is negligible compared to the diffusive one since the permeability of soils ($K \sim 10^{-10}$–10^{-13} m^2) is usually several orders of magnitude smaller than the diffusion coefficient, and the hydrostatic pressure gradient is small (~10 Pa m^{-1}). For large variations in surface pressure, this term could be important in a transitory regime (Nazaroff and Nero, 1988).

The term that governs the adsorption of radon onto solid surfaces depends on the type of material and the moisture content, and it is quantified by the coefficient k, which is usually small and negligible (Nazaroff and Nero, 1988).

Radon solubility in the aqueous phase is characterized by the Ostwald coefficient, which depends on temperature. Thus, as reflected in Clever (1979), the solubility of radon in water decreases as temperature increases, changing radon distribution between the water and air phases (Fig. 1).

2.1. Heterogeneous media. A numerical solution

The Earth's crust can be considered a porous media of finite depth resting on soil-generating rock. The diffusion coefficient of radon for rock is several orders of magnitude less than for crust, hence the transfer at the rocks–soil interface will be negligible (Nazaroff and Nero, 1988).

The diffusion coefficient varies across the soil column mainly due to moisture and temperature profiles. Under these conditions, the diffusive term is expanded so that the gradient of the diffusion coefficient also plays a part in radon transport.

$$\nabla\cdot(D_b\nabla C_{\mathrm{Rn}}) = \nabla D_b\nabla C_{\mathrm{Rn}} + D_b\nabla^2 C_{\mathrm{Rn}} \quad (6)$$

This situation has no simple analytical solution, making necessary the use of numerical techniques to get a result. To this end, a forward finite difference technique with an explicit resolution scheme (Hildebrand, 1968; Smith, 1977) has been selected. The

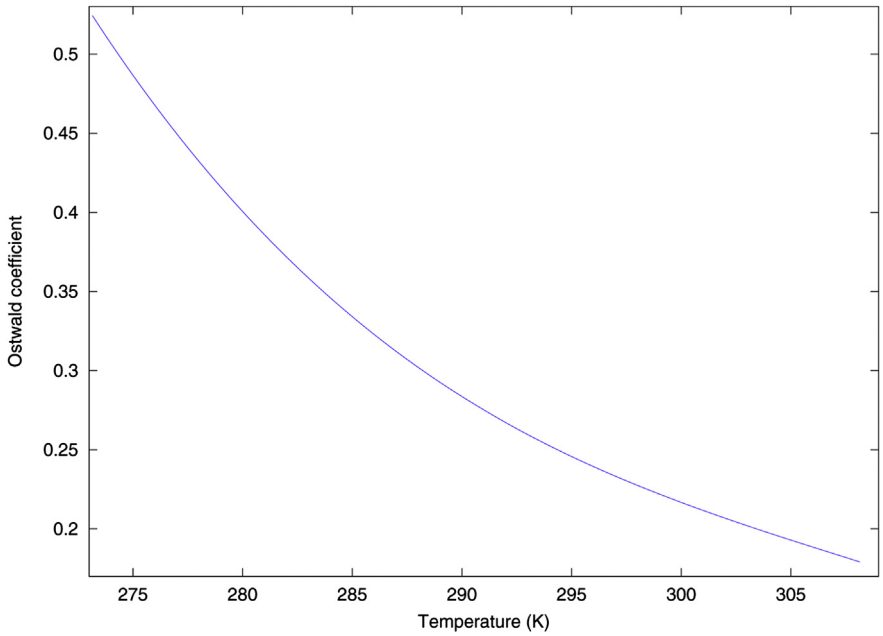

Fig. 1. Ostwald coefficient, or distribution of phases as a function of temperature for ^{222}Rn (Clever, 1979).

explicit method imposes a limitation on the convergence of the solution, in such a way that the coefficient of the second derivative (diffusion coefficient, D), the time step (dt) and spatial resolution (dx) must satisfy an algebraic relation:

$$dt < \frac{(dx)^2}{2D} \tag{7}$$

2.2. Snow cover

The existence of snow cover above the soil surface has a shielding effect on the radon flow into the free atmosphere. At steady state, the diffusion of radon through a finite layer without radon source can be described as an exponential decay modulated by the diffusion length.

Therefore, considering the snow as a porous material composed of water in solid form, it is possible to assume that the liquid water content supply to the distribution of phases is 0. In turn, the compaction of the snow cover is variable depending on the height of the column of snow and the time since deposition (Kudryashov et al., 1999). However, as an initial approach, it is possible to assume a constant porosity for the snow cover (around $p = 0.6$), and to estimate the reduction in the exhalation rate according to the snow cover thickness (Fig. 2). Under these conditions, snow cover of just half a metre thickness can lead to a 20% reduction of the exhalation rate.

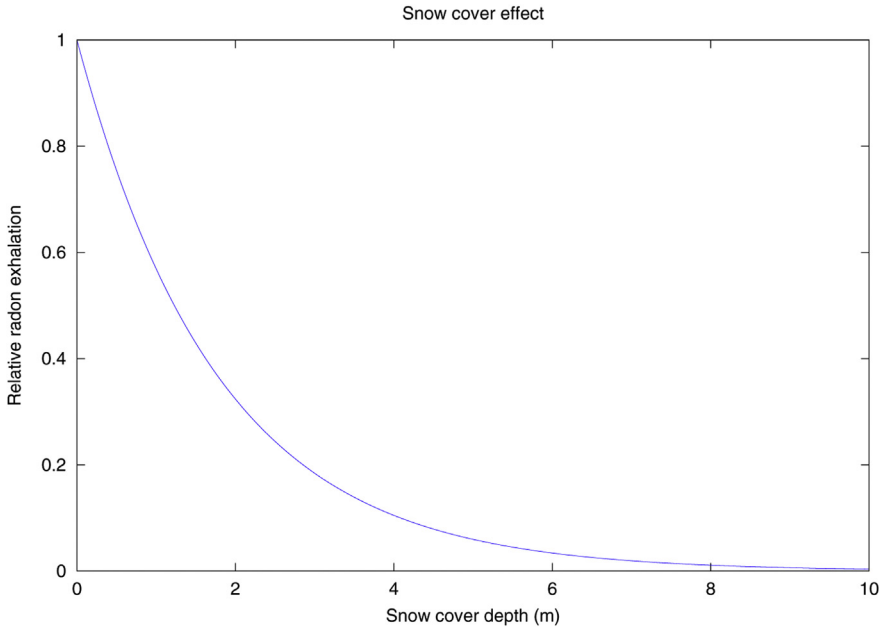

Fig. 2. Radon exhalation depending on the thickness of the snow column ($D_e = 6.6 \cdot 10^{-6}$ m^2 s^{-1}).

3. Materials and methods

3.1. Databases

3.1.1. Geochemical characterization

The activity concentration of ^{226}Ra was determined from total uranium concentration using the conversion factors proposed by the International Atomic Energy Agency (12.35 Bq kg^{-1} of ^{238}U by 1 ppm U, IAEA, 1989) and assuming that ^{226}Ra is in secular equilibrium with its parent ^{238}U.

The total U concentration was obtained from the FOREGS geochemical database (Salminen, 2006; de Vos and Tarvainen, 2006) from the Association of the Geological Surveys of The European Union. This atlas provides high quality geochemical data, containing information on 26 chemical elements analysed by ICP-MS in samples from 26 European Union countries, selected via a scheme based on a hierarchical and random mesh of 160 km^2 of the global network reference (Darnley, 1995). All sampling and analytical campaigns were conducted in order to fulfil the specifications of the IUGS/IAGC "Global Geochemical Baselines" mapping programme (Salminen, 2006; de Vos and Tarvainen, 2006). The quality of the results of this database has been tested by duplicating samples, performing routine measurement intercomparisons and analyses of reference materials.

3.1.2. Geophysical properties

The geophysical properties were derived from the Harmonized World Soil Database (HWSD) of the United Nations' Food and Agriculture Organization (FAO) in the framework of the Land Use Change and Agriculture Program (LUC), in collaboration with ISRIC-World Soil Information, the European Soil Bureau Network and the Institute of Soil Science at the Chinese Academy of Sciences.

The HWSD provides state-of-the-art information on soil characteristics and properties. This database has a spatial resolution of 0.5′ (~1 km) and more than 16,000 units of soil types. It couples the different regional databases of soil information throughout the world (SOTER, ESD, Soil Map of China, WISE) with the information contained within the FAO-UNESCO world map (FAO, 2009).

From the bulk density provided by the HWSD, the porosity of the soil units has been determined, assuming grain density = 2.65 g cm^{-3} (Cameron and Buchan, 2006).

$$p = 1 - \frac{\rho_b}{\rho_{\text{grain}}} \tag{13}$$

The emanation factor was considered constant and equal to 0.2 for all soil units and for all moisture conditions. This approach is based on the low variability of this parameter published in the literature (Ferry et al., 2002; López-Coto et al., 2009). Moreover, according to Sasaki et al. (2003) and Hassan et al., 2011, the emanation factor is significantly reduced only in cases where the humidity drops below 5%. Hence, it will not be significant in the climatological context of this work.

3.1.3. Weather variables

Monthly means, at 1° × 1° horizontal resolution, of temperature, soil moisture and snow cover thickness have been obtained from the ECMWF's global ERA-40 re-analysis database (Uppala et al., 2005).

ERA-40 is a global climate database of the atmosphere, land surface and oceans from September 1957 to August 2002. This database combines observational data from sources such as satellites, radiosondes, aircraft, etc., with a 3D model of weather forecasting using variational data-assimilation techniques, which produces accurate and consistent data.

The parametrization used in ERA-40 surface analysis to simulate soil-atmosphere and soil-vegetation interactions provides a daily water balance and energy budget for each grid cell in four layers with thicknesses of 7, 21, 72 and 189 cm.

3.2. Geographical domain, mesh and pre-processing

The extension of the selected mesh includes all EU27 countries, with a spatial resolution of 0.5′ (~1 km). A Cartesian domain was chosen between 32.5° N and 75° N latitude and −27.5° E and 45° E longitude. This configuration results in a grid of 5101 × 8701 elements. The vertical coordinate has 100 elements, covering a depth of up to two metres. The FOREGS database has been interpolated using an algorithm weighed by the inverse distance.

A global climatology for the whole period has been calculated from the monthly averages of the ERA-40 data re-analysis to obtain the average annual cycle of moisture, soil temperature and thickness of the snow cover. In addition, the results have been linearly interpolated in each layer to cover the whole horizontal coverage of the mesh.

3.3. Implementation of the transport model

A code in C++ has been written, which enables the calculation of the radon concentration profile in steady state from the data files previously conditioned, thus obtaining the exhalation rate for each horizontal cell.

The main routine reads the file and loads the necessary input variables into the memory. Then it runs along the horizontal grid executing the main subroutine for the transport model for each grid cell. Once the whole domain is covered, it writes the output in a NetCDF file.

The solver subroutine interpolates variables depending on z and calculates the diffusion coefficient for each cell in the soil profile. Then, it solves the equation of time-dependent one-dimensional transport in an iterative way until steady state is reached and the exhalation rate is calculated.

Due to the restrictions imposed by the vertical resolution ($dx = 0.02$ m) and the properties of the medium ($D \sim 10^{-6}$ m^2 s^{-1}), a safer time step $dt = 100$ s has been chosen in order to ensure stability.

The execution was carried out sequentially and automatically for each of the average months, resulting in a NetCDF file for each month that stores exhalation rates calculated for the whole domain.

4. Results

4.1. Numerical model testing

An internal validation test of the numerical model proposed has been carried out by simulating the "scenario 0" published in the international inter-comparison experiment for radon models, ERRICCA (RISO-R-1120, 1999). This scenario allows us to compare the obtained results to those provided by six laboratories through different numerical models that can be found in that report. In this way, the results can also be compared to the analytical solution obtained using the homogeneous media approach. The parameters used in this simulation are: source term, $S = 0.129749$ Bq m^{-3} s^{-1}, which describes the production of radon per unit of time and sample volume, and the effective diffusion coefficient is $D_e = 3.3 \cdot 10^{-6}$ m^2 s^{-1} ($p = 0.3$, $s = 0$).

The surface exhalation reflected in the ERRICCA report is $E_{\text{ref}} = 4.7228 \cdot 10^{-2}$ Bq m^{-2} s^{-1}. The results from the numerical solution scheme proposed in this work, $E_{\text{UHU}} = 4.7293 \cdot 10^{-2}$ Bq m^{-2} s^{-1},

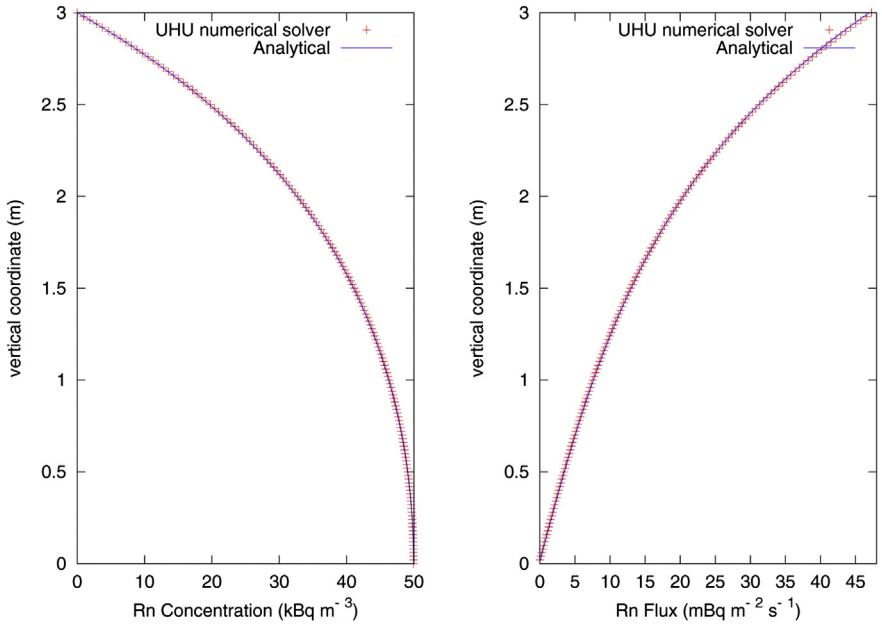

Fig. 3. Radon concentration profile (left) and radon flux profile (right) comparison between numerical and theoretical results under ERRICCA scenario 0 conditions ($De = 3.3 \cdot 10^{-6}$ m^2 s^{-1}, $S = 0.129749$ Bq m^{-3} s^{-1}; $p = 0.3$, $s = 0$).

have a relative deviation of less than 0.15% from both the reference and the analytical solution, so it can be assumed that the proposed numerical model provides satisfactory results (Fig. 3).

4.2. Radon exhalation maps, statistical parameters and probability distribution

Fig. 4 shows the radon exhalation maps for the average months of January and July for the period 1957–2002. At a glance, the wet months have a lower exhalation value mainly due to the lower radon diffusion coefficient for wet soils (Rogers and Nielson, 1991).

Table 1 details the monthly average radon exhalation, the standard deviation and the 95th and 99th percentiles for the whole geographical domain.

The wet months have lower exhalation values, around 26 Bq m^{-2} h^{-1}, underlining the influence of hydrometeorological conditions on radon exhalation. In turn, the difference between the arithmetic and geometric mean is above 9 Bq m^{-2} h^{-1} from January to April, being quite frequent values close to zero, mainly due to rainfall in winter and snow cover in northern Europe, both precluding high values of the exhalation rate. The standard deviation, 27 Bq m^{-2} h^{-1}, indicates great variability in the exhalation rate throughout the domain. In addition, the 95th percentile is below 60 Bq m^{-2} h^{-1}, and 99th is near to 100 Bq m^{-2} h^{-1}.

Dry months show higher exhalation rates than wet months, as expected. Consequently, the average value for August is 34 Bq m^{-2} h$^{-1,}$ while the minimum value (26.1 Bq m^{-2} h^{-1}) is obtained in February. The geometric mean, 27 Bq m^{-2} h^{-1}, is close to the mean, indicating a substantial reduction in values close to zero, as a consequence of seasonal rainfall reduction. The standard deviation is slightly higher than that obtained for the cold months, 28 Bq m^{-2} h^{-1}. August has the highest value for the 95th and 99th percentiles, 70 and 115 Bq m^{-2} h^{-1}, respectively.

Particularly striking is the maximum exhalation rate exceeding 1000 Bq m^{-2} h^{-1}, that results provide for a location 50 km south of Belfast (Northern Ireland). This is due to the high uranium concentration in the soil, in the range of 700 ppm of U (8 Bq g^{-1} for ^{238}U), which is far superior to that in the rest of Europe (Salminen, 2006; de Vos and Tarvainen, 2006).

Fig. 5 shows the probability distributions of radon exhalation for the months of January and July as representative of wet and dry periods. Both months show a similar functional form, with a shift of about 7 Bq m^{-2} h^{-1}, as a result of the distance between their modes. This figure also shows the existence of specific locations with unusually high exhalation rates.

4.2.1. Statistical parameters and probability distributions by region

The year probability distributions of radon exhalation rates for different regions show characteristic behaviour for each zone, depending on the local hydrological cycle and geological substrate (Fig. 6a–i).

The regional mean for Ireland (Fig. 6a) is around 75 Bq m^{-2} h^{-1} but the geometric mean of about 50 Bq m^{-2} h^{-1} shows a great asymmetry of the values distribution. The high values are connected to the relatively high ^{226}Ra contents in the substrate (55 Bq kg^{-1}). The probability distribution clearly shows two most probable values, 35 and 50 Bq m^{-2} h^{-1}, and also a core of a lower probability of occurrence, at around 95 Bq m^{-2} h^{-1}. As mentioned, the area south of Belfast contains the highest of exhalation rate both for Northern Ireland and Europe (1000 Bq m^{-2} h^{-1}).

These results are quite similar to the values of 28 and 50 Bq m^{-2} h^{-1} given by Jennings et al. (2006) for Ireland. Nevertheless, most of the sampling points were located in the northwest and southeast of the country and do not include Northern Ireland; hence no extreme value in Ireland was detected in that study.

The UK has a fairly symmetrical probability distribution (Fig. 6b). The average value is around 36 Bq m^{-2} h^{-1}, 1 Bq m^{-2} h^{-1} above the geometric mean. In turn, the standard deviation is about 10 Bq m^{-2} h^{-1}, which is similar to that found for the rest of Europe. The averaged ^{226}Ra concentration in soils (27 Bq kg^{-1}) was found to be lower than for Ireland, but higher than for meridional regions such as the Iberian Peninsula, France or Italy.

The Iberian Peninsula has average values of 25 and 45 Bq m^{-2} h^{-1} for winter and summer, respectively, and a standard deviation of 24 Bq m^{-2} h^{-1}. There are three most probable values for the Peninsula, which range from 12, 30 and 45 Bq m^{-2} h^{-1} for winter to 35, 50 and 60 Bq m^{-2} h^{-1} in summer (Fig. 6c). There is a considerable seasonal fluctuation of some 20 Bq m^{-2} h^{-1}. The P95 is

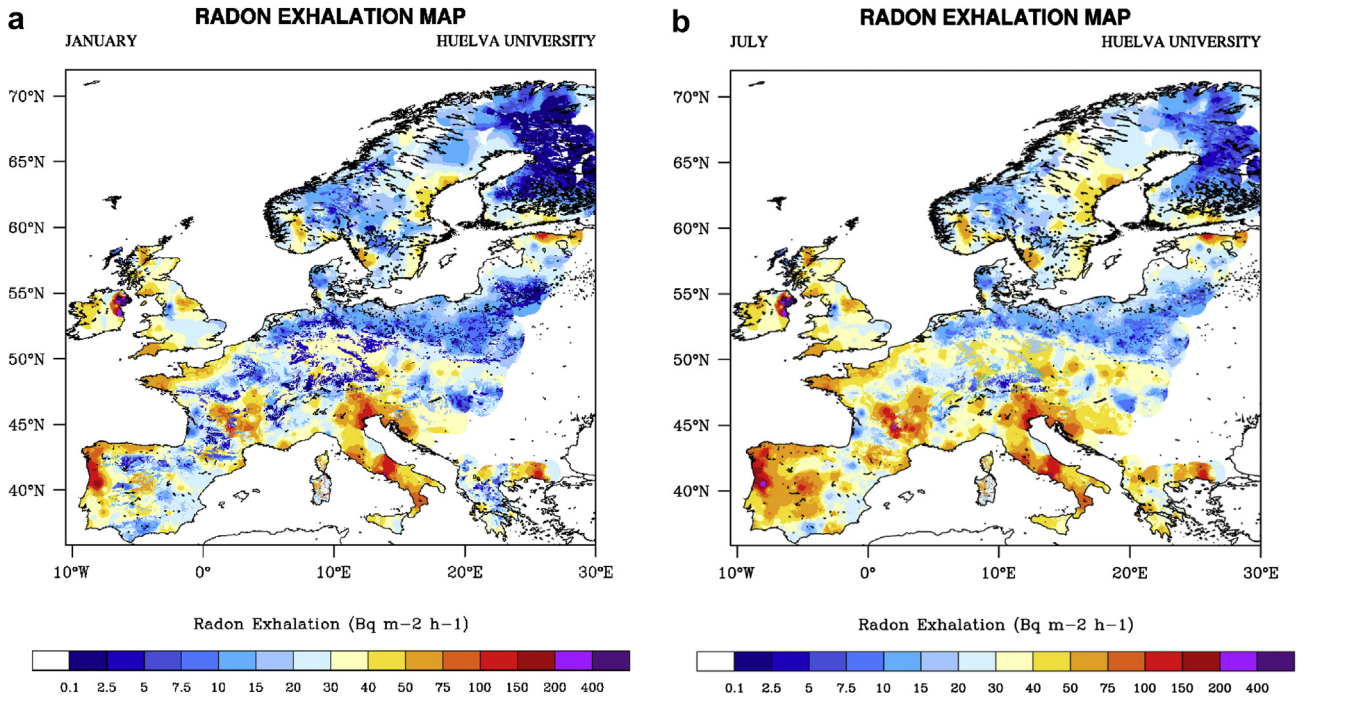

Fig. 4. a. ^{222}Rn flux map on surface (Bq m^{-2} h^{-1}) for the average month of January for the period 1957–2002. b. ^{222}Rn flux map on surface (Bq m^{-2} h^{-1}) for the average month of July for the period 1957–2002.

within a range of 80–90 Bq m^{-2} h^{-1} and the maximum is close to 220 Bq m^{-2} h^{-1} for an area located at the East of Oporto, Portugal. Clearly, the Iberian Peninsula shows great regional variability, derived from the different ^{226}Ra concentration in soils, as well as substantial seasonal fluctuations. This can be understood bearing in mind 1) the large regional differences in climate throughout the Iberian peninsula (from desert climate to Atlantic forest climate), and 2) the extreme differences between summer and winter weather conditions (in terms of rainfall and temperature), which show far higher variability than in the rest of Europe.

These results are in good agreement with those published in literature, as can be seen in Dueñas et al. (1997), with exhalation rate values between 10 and 90 Bq m^{-2} h^{-1} and a geometric mean around 35 Bq m^{-2} h^{-1}; Abril et al. (2009) with values ranging between 15 and 40 Bq m^{-2} h^{-1} for wet and dry periods respectively and Grossi et al. (2011) with a rate spectrum covering from 30 to 90 Bq m^{-2} h^{-1} for different locations.

France has a similar pattern to that of the Iberian Peninsula, derived from the combination of a similar ^{226}Ra content and a less pronounced climatic fluctuation, (Fig. 6d). The average value fluctuates around 40 Bq m^{-2} h^{-1}, with a standard deviation of 24 Bq m^{-2} h^{-1}. The P95 is between 75 and 95 Bq m^{-2} h^{-1} and the maximum ($\approx$250 Bq m^{-2} h^{-1}) occurs near the city of Cabannes. The lower seasonal variability reflects in a lower variability of soil humidity contents.

Italy has values of around 60 Bq m^{-2} h^{-1} with a standard deviation of 28 Bq m^{-2} h^{-1}. The P95 is 115 Bq m^{-2} h^{-1}, being hence highly probable to find elevated values of the exhalation rate. These high values are due to the relatively high ^{226}Ra content, 40 Bq kg^{-1}. In detail, the probability distribution (Fig. 6e) reveals a multimodal pattern with a clear maximum ($\approx$45 Bq m^{-2} h^{-1}). Exhalation rates below 25 Bq m^{-2} h^{-1} are associated to a very low occurrence probability. The pattern is completed by a narrow peak located at 75 Bq m^{-2} h^{-1} with a high probability of occurrence, and two low probability additional peaks at 85 and 120 Bq m^{-2} h^{-1}.

The exhalation rate in Germany is relatively small with average values ranging from 21 to 26 Bq m^{-2} h^{-1} and a standard deviation of 12 Bq m^{-2} h^{-1}. That is connected to the relatively low ^{226}Ra contents (26 Bq kg^{-1}). The distribution of values is clearly affected by seasonal variation. The distribution shows a high probability of occurrence for values near 3 Bq m^{-2} h^{-1} during the winter, being replaced this maximum during the warm season by drastically less prominent local maximum around 20 Bq m^{-2} h^{-1}. Above these values, a separate core with a high probability of occurrence is located within the 35–40 Bq m^{-2} h^{-1} range, which agrees with the P95. On the other hand, the maximum does not exceed 50 Bq m^{-2} h^{-1} (Fig. 6f). According to Dörr and Münich (1990), the experimental probability distribution for western Germany shows two most probable values, 25 and 66 Bq m^{-2} h^{-1}, which are slightly higher than the model-predicted maxima.

The probability distribution for the countries of Eastern Europe (Fig. 6g) is very similar to that of Germany, although it is dominated by exhalation rate values around 15 Bq m^{-2} h^{-1}, instead the 35–40 Bq m^{-2} h^{-1} range found in Germany. The average ranges from 17 to 21 Bq m^{-2} h^{-1} with a standard deviation of 11 Bq m^{-2} h^{-1}. Again, the P95 is around 35–40 Bq m^{-2} h^{-1}, but reaches maximum values

Table 1
European domain statistical parameters (Bq m^{-2} h^{-1}).

	Arithmetic mean	Geometric mean	Standard deviation	P95	P99
January	26.7	17.6	27.1	59.2	101.6
February	26.1	15.9	27.2	58.6	101.2
March	26.3	15.6	27.4	59.4	102.4
April	26.3	17.1	27.1	58.9	101.7
May	30.1	22.8	27.5	63.4	105.9
June	31.9	25.8	27.7	66.1	109.2
July	33.3	27.1	28.4	69.2	113.8
August	33.6	27.2	28.4	69.7	114.4
September	32.6	26.2	27.9	67.6	111.3
October	31.2	24.9	27.2	64.6	107.2
November	29.5	22.8	27.1	61.9	104.3
December	27.9	20.3	27.1	60.4	102.6

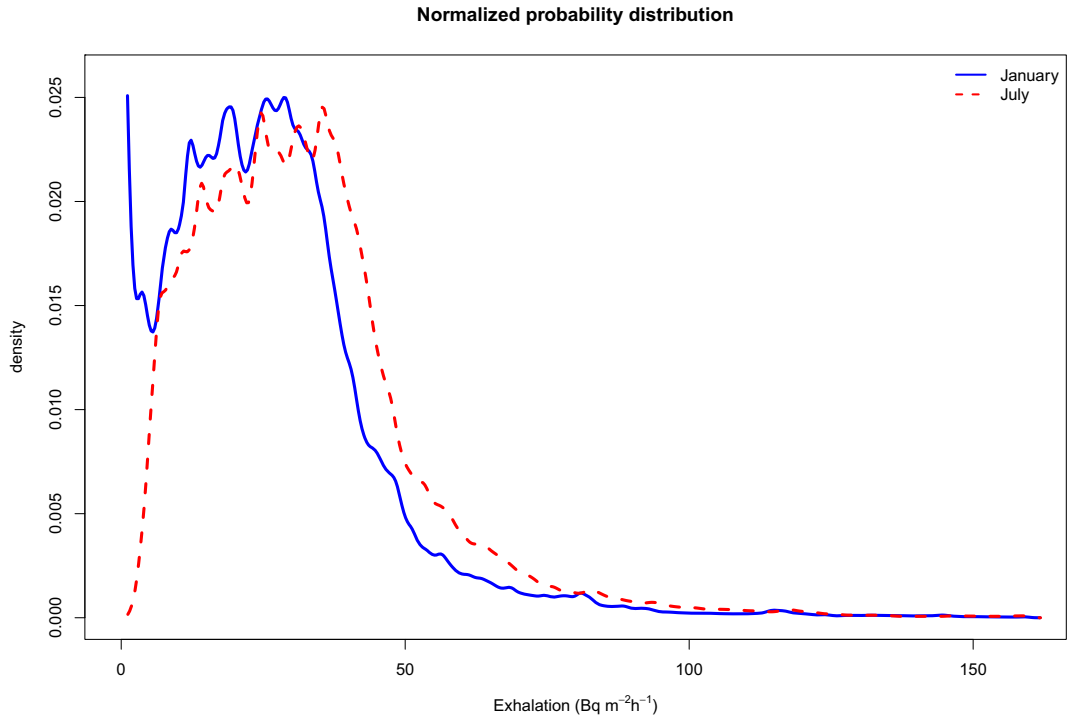

Fig. 5. Probability distribution of the exhalation rate of the entire domain for the averaged months January and July for the period 1957–2002.

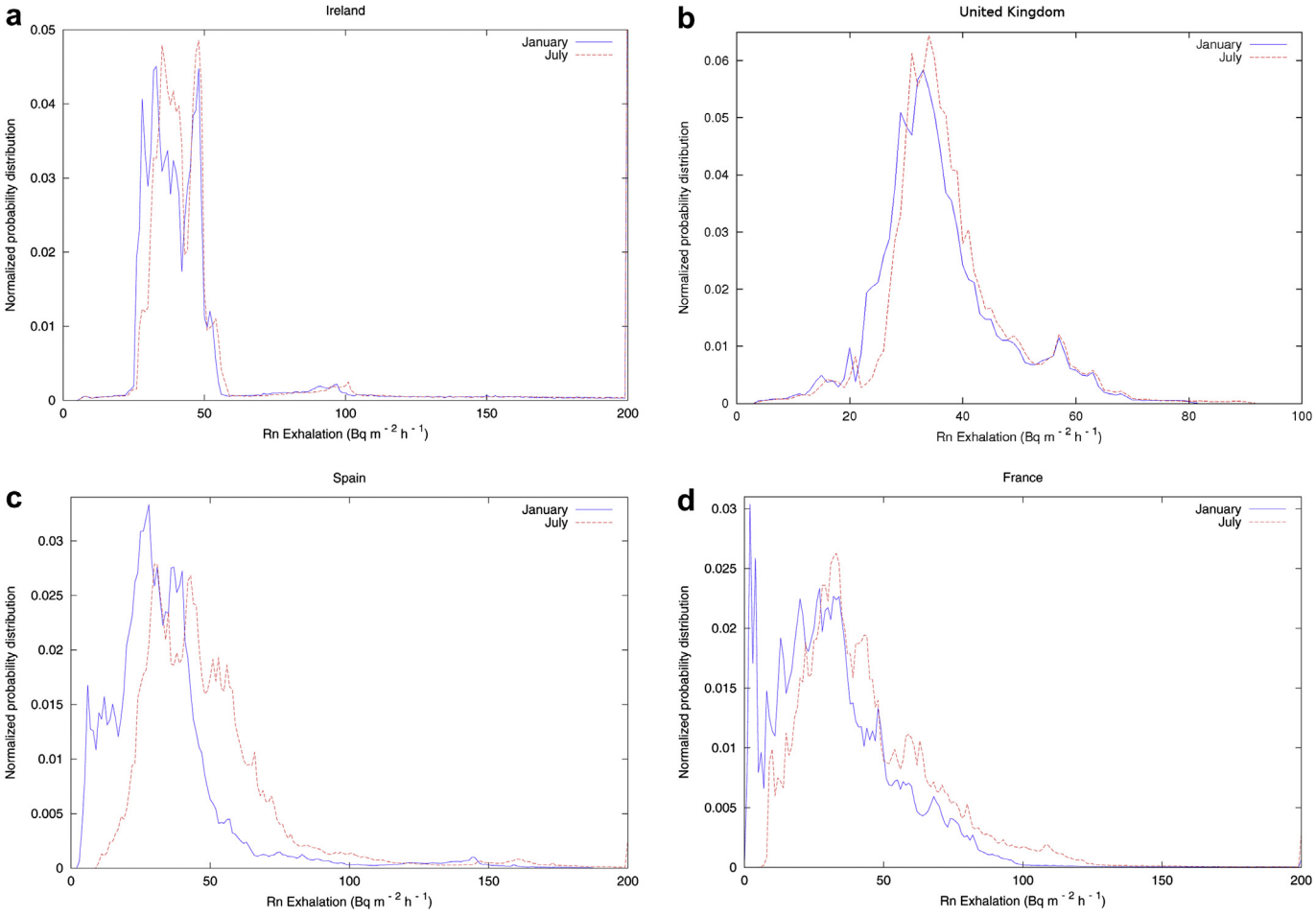

Fig. 6. Regional probability distribution. a) Ireland, b) UK, c) Spain, d) France, e) Italy, f) Germany, g) Eastern Europe, h) Scandinavian countries, i) Finland.

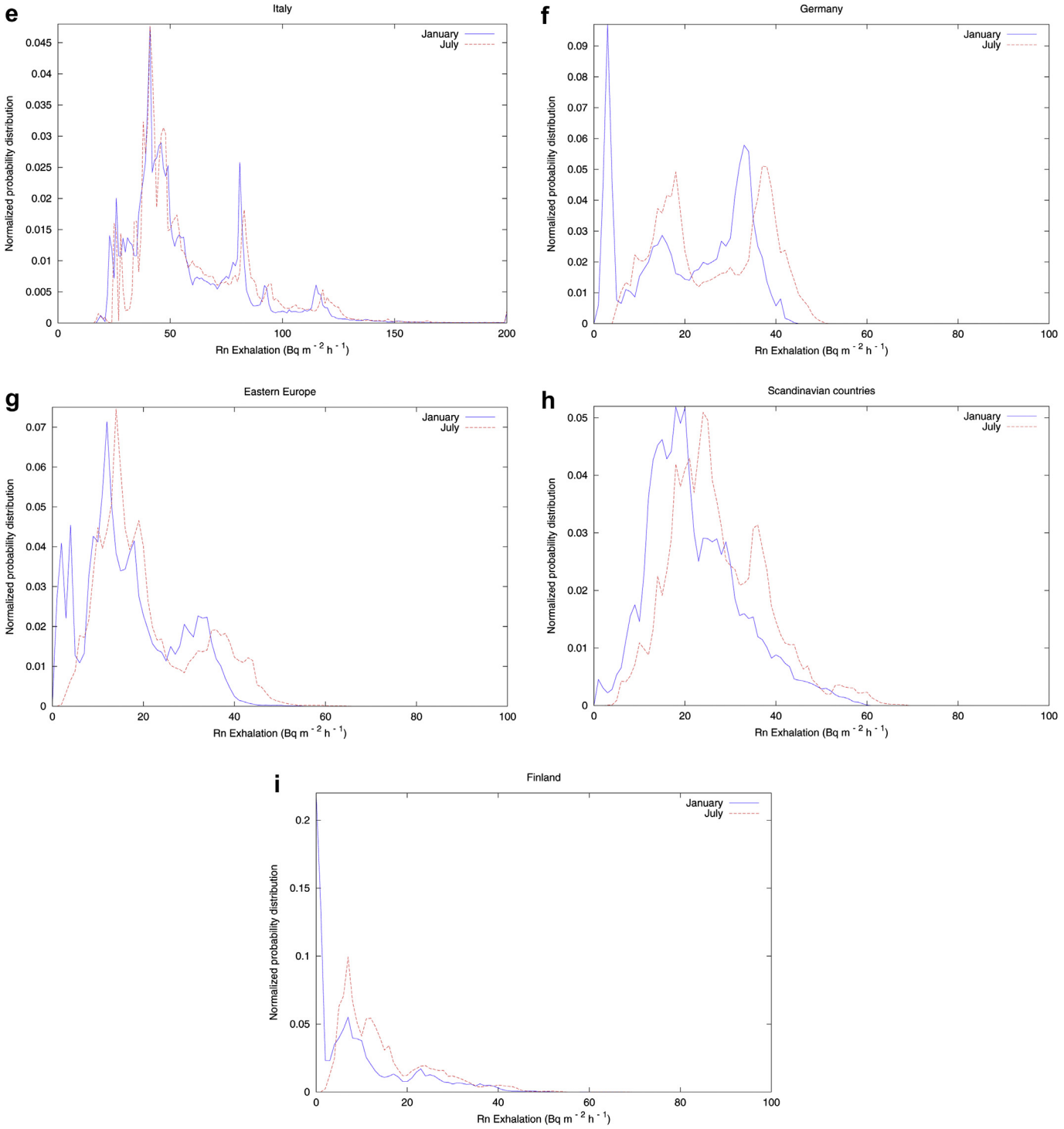

Fig. 6. (*continued*).

of about 65 Bq m^{-2} h^{-1}. The fact that the values here found are below those found in Germany sems to be in agreement with the smallest ^{226}Ra concentration (in the range of 20 Bq kg^{-1} in average against 26 Bq kg^{-1}).

The Scandinavian Peninsula has values of around 25 Bq m^{-2} h^{-1} with a standard deviation of 10 Bq m^{-2} h^{-1} and a seasonal fluctuation of some 5 Bq m^{-2} h^{-1}. The P95 reaches 45 Bq m^{-2} h^{-1} and the maximum does not exceed 70 Bq m^{-2} h^{-1} (Fig. 6h).

Finland has the lowest values in Europe, with an average of 9 Bq m^{-2} h^{-1} for winter and 15 Bq m^{-2} h^{-1} for summer (Fig. 6i). Furthermore, the averaged ^{226}Ra content is around 15 Bq kg^{-1}, which explains the low exhalation average. Specifically, the low geometric mean value, 3 Bq m^{-2} h^{-1}, indicates high values close to zero. This fact is due to, as previously explained, the presence of a snow cover during most of the year. The standard deviation is around 10 Bq m^{-2} h^{-1} and the P95 stands at about 33 Bq m^{-2} h^{-1}.

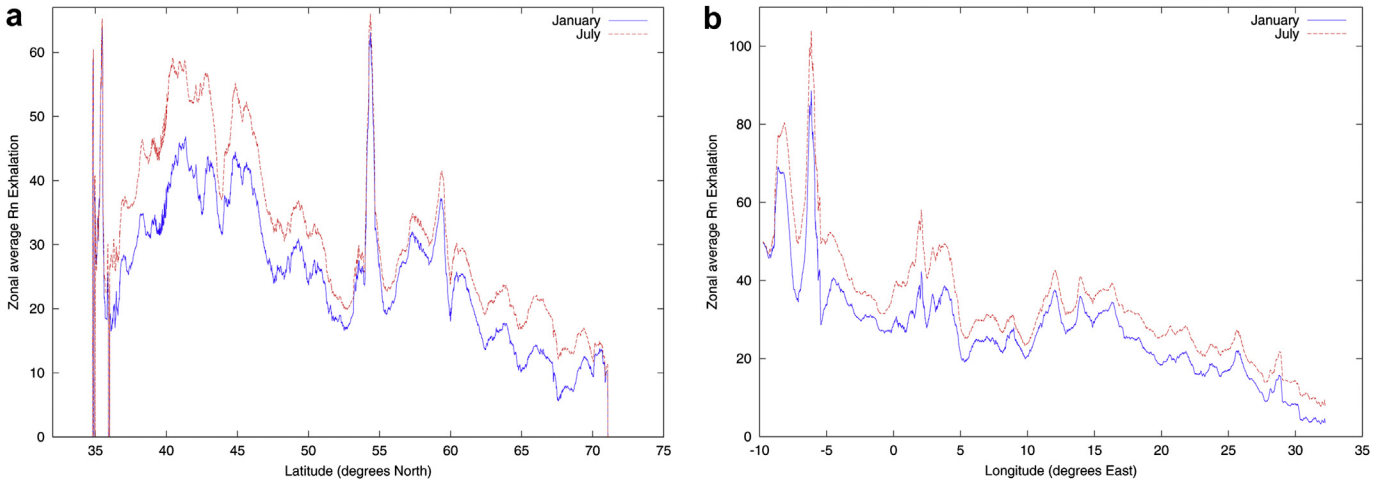

Fig. 7. Zonal mean. a) Latitude, b) Longitude.

Despite these values the maximum is 80 Bq m^{-2} h^{-1}, showing high exhalation locations in the South, near Helsinki.

According to Szegvary et al. (2007), Finland has two different areas: the north, with an average value of 30 Bq m^{-2} h^{-1}, which is twice the value predicted in this work for the average summer; and the south, which has higher values, around 100 Bq m^{-2} h^{-1}, which are consistent with the results predicted. It could be argued that the magnitude of differences found for the North region could be explained by the fact that the snows cover (which presence is highly probable at the North) fairly reduces the radon exhalation, although the reduction of gamma dose rate is less pronounced. Under these conditions, it can be understood that a proxy based on gamma dose rate measurements could overestimate the exhalation rate at regions covered by snow.

In general, the averaged exhalation values for each region are due to the geological substrate since the ^{226}Ra is driving the radon generation; nevertheless, the soil humidity content is the fundamental factor affecting the seasonal variability.

Besides, the mean values calculated by the model for the dry period reproduce the results of the measurements. However, the deviation of model-predicted values from the experimental values increases as the experimental value grows, showing the smoothing effect of the climatological component of the obtained map.

4.3. Comparison with other European models of radon exhalation

Due to the scarcity of direct measurements of radon flux at the surface, several authors have proposed different alternatives for

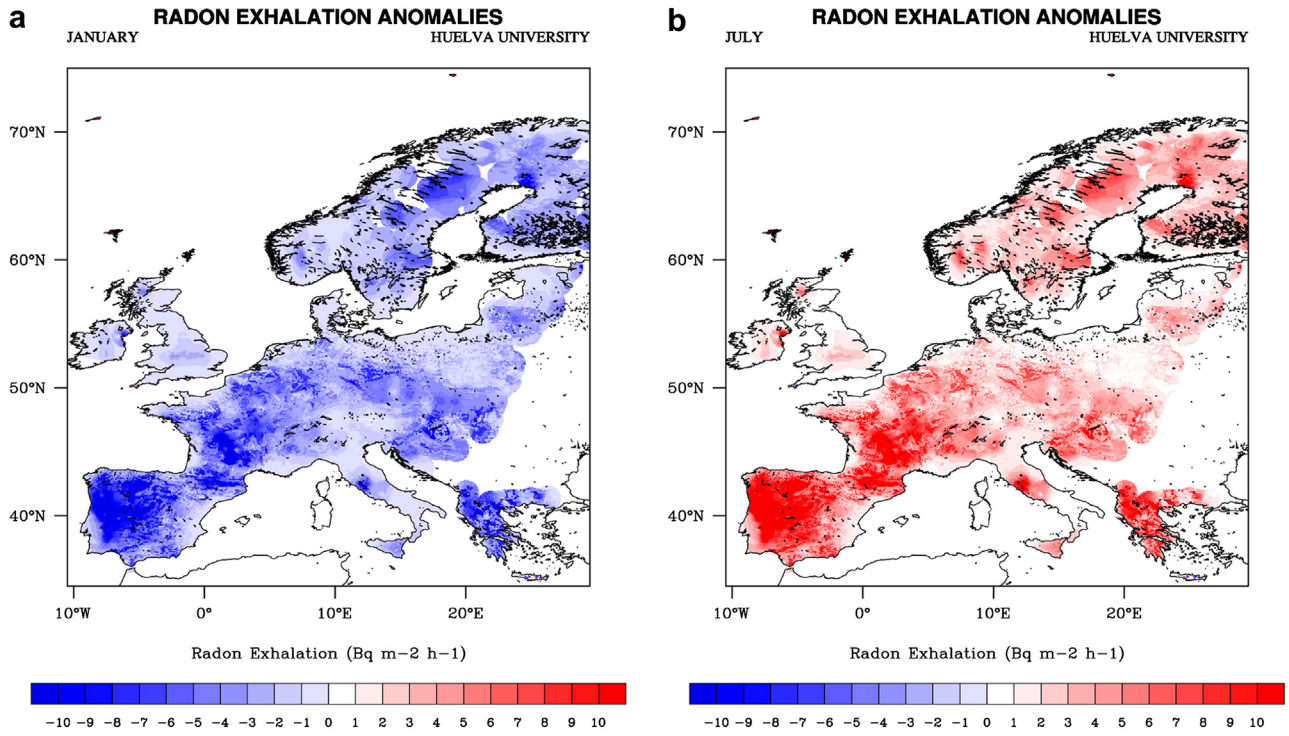

Fig. 8. Local mean deviations. a) January, b) July.

estimating radon exhalation in Europe. Rasch et al. (2000) proposed a global exhalation value of around 75 Bq m^{-2} h^{-1} for between 30° and 60° N, and 33 Bq m^{-2} h^{-1} for higher latitudes. Conen and Robertson (2002) suggested that the flow of radon may decrease linearly from 75 Bq m^{-2} h^{-1} at 30° N to 15 Bq m^{-2} h^{-1} at 70° N.

Fig. 7 shows the zonal average for January and July. Exhalation increases on average from 25 to 50 Bq m^{-2} h^{-1} between 35° and 42° N, followed by a non-linear decrease to 15 Bq m^{-2} h^{-1} for 70° N.

At 53° N, there is a rather narrow maximum which exposes the existence of outliers in these latitudes. It is clear that the latitudinal trend suggested by Conen and Robertson (2002) agrees with the results calculated by the model. However, for latitudes below 42° N, their proposal overestimates the results calculated with the proposed model. On the other hand, the zonal mean decreases as a function of longitude from West to East. The maximum values correspond to longitudes between 5° and 10° W, where two peaks above 60 and 80 Bq m^{-2} h^{-1} appear at 8° and 5.2° W respectively.

Szegvary et al. (2009) present a radon flux map derived from correlations between the exhalation rate and the external radiation dose obtained experimentally in a previous work (Szegvary et al., 2007). The global average for Europe presented by this map is around 38 Bq m^{-2} h^{-1}, higher than the 30 Bq m^{-2} h^{-1} obtained in this work, and the standard deviation is about 15 Bq m^{-2} h^{-1}, less than the value of 27 Bq m^{-2} h^{-1} shown in this work. The referred approximation provides, almost systematically, exhalation values higher than those obtained with the model proposed in this paper. Thus, the regional averages for the United Kingdom, 50 Bq m^{-2} h^{-1}, Spain, 77 Bq m^{-2} h^{-1}, France, 45 Bq m^{-2} h^{-1}, Germany, 39 Bq m^{-2} h^{-1} and Finland, 22 Bq m^{-2} h^{-1}, are higher than those discussed in the previous section. The largest deviation was found for the Iberian Peninsula, for which Szegvary's approximation overestimates the exhalation values respecting to measured values, Grossi et al. (2011) In this work is shown that the gamma dose rate data used as input in the flux estimation are too high because they are uncorrected values. Nevertheless, after applying the corrections proposed by Sáez Vergara et al. (2002), those data could be used in order to obtain better radon flux estimations.

4.4. Local mean deviations. Annual cycle

Fig. 8 shows the absolute deviations of the local mean for January (wet season) and July (dry season). Obviously, during the wet months the entire domain has values below the local mean and, in turn, the dry period has positive deviations in the whole domain. Lower latitudes systematically exhibit the largest deviations, showing wider fluctuations. Hence, in certain locations in the Iberian Peninsula and France, the seasonal variation easily exceeds 30 Bq m^{-2} h^{-1}, in agreement with the previously mentioned extreme weather fluctuations for such regions. The higher latitudes show low seasonal fluctuations due to lower amplitude in the hydrological cycle in the soil.

In order to compare the annual cycle and the seasonal fluctuations of the exhalation rate, four interesting locations throughout the European continent have been chosen (Fig. 9). The northern locations have their maximum exhalation in July, while the meridional locations peak in August. In turn, eastern locations have their lowest exhalation rate in March, and western locations does it in April.

The effect of snow cover largely determines the exhalation in areas like Lappi, Finland. As an example, Fig. 9 shows that fluxes around zero are reached during the colder months mainly due to snow cover, which has a double effect; shielding the exhalation of radon on the surface and keeping the soil wet underneath. This combined effect gives snow cover an important role in the seasonal fluctuations of exhalation.

4.5. Constraints and sources of error

Clearly, the approximations made in the model impose some limitations on the results in this paper. The one-dimensional nature

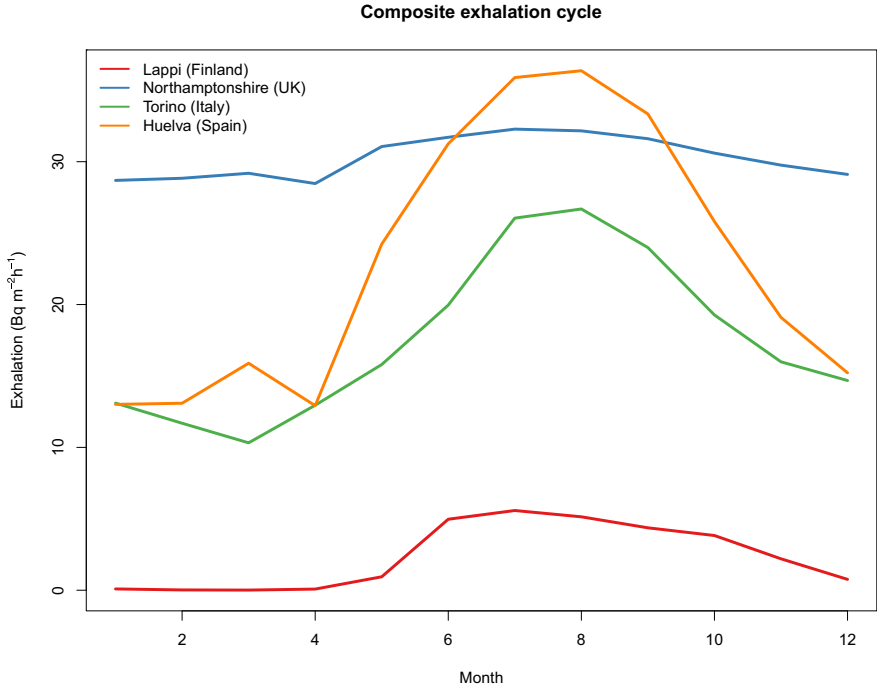

Fig. 9. Exhalation annual cycle for Lappi (Finland), Northamptonshire (United Kingdom), Torino (Italy) and Huelva (Spain).

of the model does not enable evaluation of the horizontal diffusive fluxes that may occur between different areas. Furthermore, consideration of a constant emanation factor could lead to 50% uncertainty in the source term of certain extremely dry soils. Also, the porosity homogeneity in the snow cover can only be assumed for climatological purposes. Its dynamic nature, which modifies compaction as a function of thickness and time elapsed from deposition, makes it highly probable that the screening effect is understated. The frost has not been included due to the nature of the simple snow cover model and the available data. Nevertheless, the frost could cause a percentual exhalation diminishing mainly in wet soils, which have a low exhalation themselves. This fact implies the net exhalation error should be low.

Cracks and fractures existing in the soil have not been taken into account since the diffusive nature of the model. This fact could affect the exhalation in highly cracked soils such as volcanic regions and Scandinavian areas, where the ice could enhance the soil and rock fractures.

The resolution and accuracy of data inventories largely determine the uncertainties and goodness of the results. Thus, the required horizontal interpolations limit an extension of the final resolution of the results. That makes necessary to include inventories that have enhanced spatial resolution.

5. Conclusions

A numerical model of radon transport in finite, heterogeneous and porous media has been developed to calculate the exhalation rate of European soils by using geological, geochemical and climatological parameters.

The theoretical model is based on the fundamental equation of radon transport in porous media, with the transport coefficient dependent on temperature and humidity. It also includes a simple model that evaluates the effect of snow cover.

A climatology of radon exhalation has been produced and the average values, the probability distributions, seasonal variability and an European high resolution radon exhalation monthly average have been obtained. The results have been compared to experimental measurements of radon flux in the literature, showing a general good agreement.

The results vary greatly depending on the location and the season of the year, with a spatial standard deviation of around the annual average value (30 Bq m^{-2} h^{-1}). In turn, the seasonal deviation is around 25% the annual average value. Systematically lower latitudes exhibit the largest deviations, with greater amplitude in seasonal fluctuations. The asymmetry of the results around the mean value reveals the existence of specific locations with unusually high exhalations. The detailed probability distributions for specific regions show different behaviour patterns for each zone, depending on the hydrological cycle and geological substrate.

The calculated inventory can be easily integrated into atmospheric transport models and also serves as a high-resolution baseline for policy decisions regarding the determination of areas of high risk of exposure to radon. The gridded data are available for the scientific community upon request.

Appendix A. Supplementary data

Supplementary data related to this article can be found at http://dx.doi.org/10.1016/j.atmosenv.2013.02.043.

References

Abril, J.M., García-Tenorio, R., Periañez, R., Enamorado, S.M., Andreu, L., Delgado, A., 2009. Occupational dosimetric assessment (inhalation pathway) from the application of phosphogypsum in agriculture in South West Spain. Journal of Environmental Radioactivity 100, 29–34.

Bousquet, P., Ciais, P., Miller, J.B., Dlugokencky, E.J., Hauglustaine, D.A., Prigent, C., van der Werf, G., Peylin, P., Brunke, E., Carouge, C., Langenfelds, R.L., Lathiere, J., Papa, F., Ramonet, M., Schmidt, M., Steele, L.P., Tyler, S.C., White, J.W.C., 2006. Contribution of anthropogenic and natural sources methane emissions variability. Nature 443, 439–443.

Cameron, K.C., Buchan, G.D., 2006. Porosity and pore size distribution. In: Encyclopedia of Soil Science. Taylor and Francis, London, pp. 1350–1353.

Clever, H.L., 1979. Solubility Data Series. In: Krypton, Xenon and Radon – Gas Solubilities, vol. 2. Pergamon Press.

Conen, F., Robertson, L.B., 2002. Latitudinal distribution of radon-222 flux from continents. Tellus 54 (B), 127–133.

Darnley, A.G., 1995. A Global Geochemical Database for Environmental and Resource Management. UNESCO, Paris. Final report of IGCP Project 259.

de Vos, W., Tarvainen, T., 2006. Geochemical Atlas of Europe Part 2: Interpretation of Geochemical Maps, Additional Tables, Figures, Maps and Related Publications. In: Geochemical Atlas of Europe, vol. 2. EuroGeosurveys and Foregs, Espoo, Finland.

Dentener, F., Feichter, J., Jeuken, A., 1999. Simulation of the transport of Rn-222 using on-line and off-line global models at different horizontal resolutions: a detailed comparison with measurements. Tellus 51 (B), 573–602.

Dörr, H., Münich, K.O., 1990. Radon flux and soil air concentration profiles in West Germany. Soil ^{222}Rn as tracer for gas transport in the unsaturated soil zone. Tellus 42B, 20–28.

Dueñas, C., Fernandez, M.C., Carretero, J., Liger, E., Perez, M., 1997. Release of ^{222}Rn from some soils. Annales Geophysicae 15, 124–133.

FAO/IIASA/ISRIC/ISSCAS/JRC, 2009. Harmonized World Soil Database (version 1.1). FAO, Rome, Italy and IIASA, Laxenburg, Austria.

Ferry, C., Richon, P., Beneito, J., Cabrera, J., Sabroux, C., 2002. An experimental method for measuring the radon-222 emanation factor in rocks. Radiation Measurements 35, 579–583.

Griffiths, A.D., Zahorowski, W., Element, A., Werczynski, S., 2010. A map of radon flux at the Australian land surface. Atmospheric Chemistry and Physics 10, 8969–8982.

Grossi, C., Vargas, A., Camacho, A., López-Coto, I., Bolivar, J.P., Xia, I., Conen, F., 2011. Intercomparison of different direct and indirect methods to determines ^{222}Rn flux from soils. Radiation Measurements 46, 112–118.

Gurney, K.R., Law, R.M., Denning, A.S., Rayner, P.J., Baker, D., Bousquet, P., Bruhwiler, L., Chen, Y.H., Ciais, P., Fan, S., Fung, I.Y., Gloor, M., Heimann, M., Higuchi, K., John, J., Maki, T., Maksyutov, S., Masarie, K., Peylin, P., Prather, M., Pak, B.C., Randerson, J., Sarmiento, J., Taguchi, S., Takahashi, T., Yuen, C.W., 2002. Towards robust regional estimates of CO_2 sources and sinks using atmospheric transport models. Nature 415, 626–630.

Hassan, N.M., Ishikawa, T., Hosoda, M., Iwaoka, K., Sorimachi, A., Sahoo, S.K., Janik, M., Kranrod, C., Yonehara, H., Fukushi, M., Tokonami, S., 2011. The effect of water content on the radon emanation coefficient for some building materials used in Japan. Radiation Measurements 46 (2), 232–237.

Hildebrand, F.B., 1968. Finite-difference Equations and Simulations, Section 2.2. Prentice-Hall, Englewood Cliffs, New Jersey.

IAEA, 1989. International Atomic Energy Agency; Construction and Use of Calibration Facilities for Radiometric Field Equipment. IAEA, Vienna. Technical Reports Series No. 309.

Jacob, D.J., Prather, M.J., Rasch, P.J., Shia, R.L., Balkanski, Y.J., Beagley, S.R., Bergmann, D.J., Blackshear, W.T., Brown, M., Chiba, M., Chipperfield, M.P., deGrandpre, J., Dignon, J.E., Feichter, J., Genthon, C., Grose, W.L., Kasibhatla, P.S., Kohler, I., Kritz, M.A., Law, K., Penner, J.E., Ramonet, M., Reeves, C.E., Rotman, D.A., Stockwell, D.Z., VanVelthoven, P.F.J., Verver, G., Wild, O., Yang, H., Zimmermann, P., 1997. Evaluation and intercomparison of global atmospheric transport models using Rn-222 and other short-lived tracers. Journal of Geophysical Research 102, 5953–5970.

Jennings, S.G., Ciais, P., Biraud, S., Ramonet, M., 2006. Environmental RTDI Programme 2000–2006, Irish Greenhouse Gas Emissions. Environmental Protection Agency, Ireland. Final Report, Technical Report.

Kudryashov, N.A., Alekseeva, I.K., Nagornov, O.V., 1999. Formation of a snow-firn layer in surface melting of snow. Journal of Engineering Physics and Thermophysics 72, 1099–1106.

López-Coto, I., Mas, J.L., Bolivar, J.P., García-Tenorio, R., 2009. A short-time method to measure the radon potential of porous materials. Applied Radiation and Isotopes 67, 133–138.

Nazaroff, W., Nero, A.V., 1988. Radon and Its Decay Products in Indoor Air. John Wiley & Sons, New York.

Porstendöfer, J., 1994. Properties and behaviour of radon and thoron and their decay products in the air. Journal Aerosol Science 25, 219–263.

Rasch, P., Feichter, J., Law, K., Mahowald, N., Penner, J., Benkovitz, C., Genthon, C., Giannakopoulos, C., Kasibhatla, P., Koch, D., Levy, H., Maki, T., Prather, M., Roberts, D.L., Roelofs, G.-J., Stevenson, D., Stockwell, Z., Taguchi, S., Kritz, M., Chipperfield, M., Baldocchi, D., McMurry, P., Barrie, L., Balkanski, Y., Chatfield, R., Kjellstrom, E., Lawrence, M., Lee, H.N., Lelieveld, J., Noone, K.J., Seinfeld, J., Stenchikov, G., Schwartz, S., Walcek, C., Williamson, D., 2000. A comparison of scavenging and deposition processes in global models: results from the WCRP Cambridge Workshop of 1995. Tellus 52 (B), 1025–1056.

RISO-R-1120, 1999. ERRICCA Radon Model Intercomparison Exercise. RISO National Laboratory, Roskilde, Denmark.

Rogers, V.C., Nielson, K.K., 1991. Multiphase radon generation and transport in porous media. Health Physics 60, 807–815.

Sáez Vergara, J.C., Romero Gutiérrez, A.M., Rodríguez Jiménez, R., 2002. Resumen de las medidas comparadas en las estaciones de REVIRA. In: Acuerdo Especifico CIEMAT-CSN 97/187 sobre Optimización de la calidad en la explotación de la red REVIRA. Madrid.

Salminen, 2006. Geochemical atlas of Europe part 1: background information, methodology and maps. In: Salminen, T. (Ed.), Geochemical Atlas of Europe, vol. 1. EuroGeosurveys and Foregs, Espoo, Finland.

Sasaki, T., Gunji, Y., Okuda, T., 2003. Mathematical modelling of radon emanation. Journal of Nuclear Science and Technology 41 (142), 151.

Schery, S.D., Wasiolek, M., 1998. Modeling Radon Flux from the Earth's Surface. In: Radon and Thoron in the Human Environment. World Scientific, Singapore, pp. 207–217.

Smith, G.D., 1977. Numerical Solution of Partial Differential Equations: Finite Difference Methods. Oxford University Press (Clarendon), London and New York.

Szegvary, T., Leuenberger, M.C., Conen, F., 2007. Predicting terrestrial ^{222}Rn flux using gamma dose rate as a proxy. Atmospheric Chemistry and Physics 7, 2789–2795.

Szegvary, T., Conen, F., Ciais, P., 2009. European ^{222}Rn inventory for applied atmospheric studies. Atmospheric Environment 43, 1536–1539.

Uppala, S.M., KÅllberg, P.W., Simmons, A.J., Andrae, U., Da Costa Bechtold, V., Fiorino, M., Gibson, J.K., Haseler, J., Hernandez, A., Kelly, G.A., Li, X., Onogi, K., Saarinen, S., Sokka, N., Allan, R.P., Andersson, E., Arpe, K., Balmaseda, M.A., Beljaars, A.C.M., Van De Berg, L., Bidlot, J., Bormann, N., Caires, S., Chevallier, F., Dethof, A., Dragosavac, M., Fisher, M., Fuentes, M., Hagemann, S., Hólm, E., Hoskins, B.J., Isaksen, L., Janssen, P.A.E.M., Jenne, R., McNally, A.P., Mahfouf, J.F., Morcrette, J.J., Rayner, N.A., Saunders, R.W., Simon, P., Sterl, A., Trenberth, K.E., Untch, A., Vasiljevic, D., Viterbo, P., Woollen, J., 2005. The ERA-40 re-analysis. Quarterly Journal of the Royal Meteorological Society 131 (612), 2961–3012.